

B-physics in ATLAS

V.Nikolaenko on behalf of the ATLAS Collaboration^{*†}

Institute for High Energy Physics, 142281, Protvino, Moscow region, Russia

E-mail: Vladimir.Nikolaenko@cern.ch

Abstract. A survey of B-physics and quarkonium production studies in ATLAS experiment[1] is presented, on the data acquired from pp interactions at $\sqrt{s} = 7\text{TeV}$ at LHC. A new bottomonium state, the $\chi_b(3P)$ has been discovered. Differential cross sections of prompt and non-prompt J/ψ production are measured. Also, the cross sections of $\Upsilon(1S)$, $\Upsilon(2S)$ and $\Upsilon(3S)$ are measured. The production cross section of b -hadrons is determined through semileptonic decays with muons. Precise measurements of Λ_b baryon mass and lifetime are performed. A limit on branching ratio for decay channel $B_s \rightarrow \mu + \mu^-$ is set, the CP -violating parameter ϕ_s and the lifetime difference between CP - even and CP -odd B_s decays are measured in the channel $B_s \rightarrow J/\psi\phi(1020)$.

LHC on the March - IHEP-LHC,

20-22 November 2012

Institute for High Energy Physics, Protvino, Moscow region, Russia

^{*}Speaker.

[†]

1. Introduction

Dimuon triggers are the main working tool of the B-Physics group for selection pp -collisions of interest. Many processes of interest have di-lepton final states, or di-lepton plus additional soft object, photon or track(s). At relatively small transverse momenta, dimuons provide significantly better mass resolution and a clean trigger in comparison with electrons. Trigger pattern for dimuon candidates in J/ψ and Υ regions is shown in Fig.1. The J/ψ , $\psi(2s)$ and $\Upsilon(1S)$ signals are clearly seen. Events with dimuon mass between charm and bottom onia are triggered also, which provides statistics for search of $B_s \rightarrow \mu^+ \mu^-$ decay.

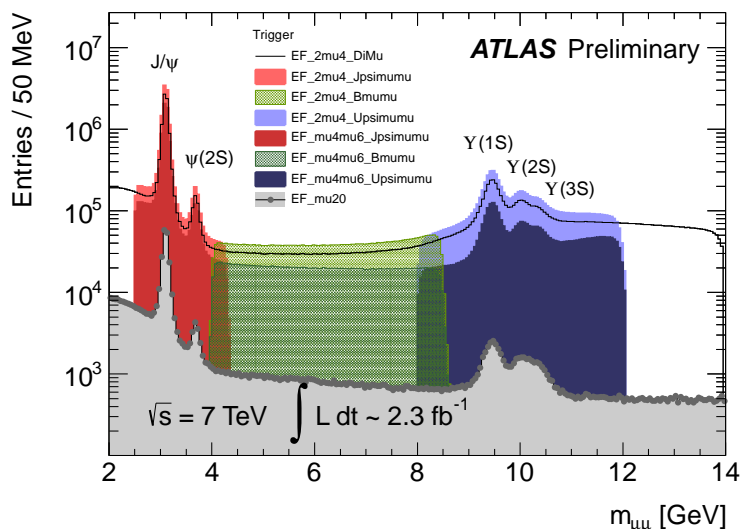


Figure 1: Invariant mass spectrum of oppositely charged muon candidate pairs for different triggers at the beginning of 2011 data taking[2]. Notation $EF_2mu4_Jpsimumu$ means the Event Filter trigger for two muons in J/ψ mass region, both muons with p_t greater than 4 GeV . Notation EF_mu20 means the Event Filter trigger for single muon with p_t greater than 20 GeV .

CP-violation and rare decay studies are based on low-pt dimuon triggers. Some studies are based on a single muon triggers. In 2011 run, the the dimuon triggers with p_t of both muons greater than 4 GeV had no prescale. With the rise of instantaneous luminosity in 2012 data taking at $\sqrt{s} = 8\text{ TeV}$, the trigger requirements become significantly tighter. The dimuon triggers with p_t of both muons greater than 4 GeV have been prescaled by a factor > 10 at the first level trigger. At instantaneous luminosity greater or equal $L = 5.0 \times 10^{33}$, unprescaled triggers have been kept with requirements on p_t of one muon greater than 6 GeV and p_t of second muon greater than 4 GeV or 6 GeV , depending on current luminosity. Data acquired with prescaled dimuon triggers were written into a separate data stream, so called Delayed Stream.

B-physics analyses based mainly on combined muons (i.e. reconstructed in Inner Detector plus Muon Spectrometer), with muon transverse momentum greater than 4 GeV and with small impact parameters with respect to the primary vertex. Some analyses use specific triggers with one or two muons in the Barrel (pseudorapidity $|\eta| < 1.2$), there is a better reconstruction precision and less background in comparison with Endcaps ($1.2 < |\eta| < 2.5$). Some analyses accept also

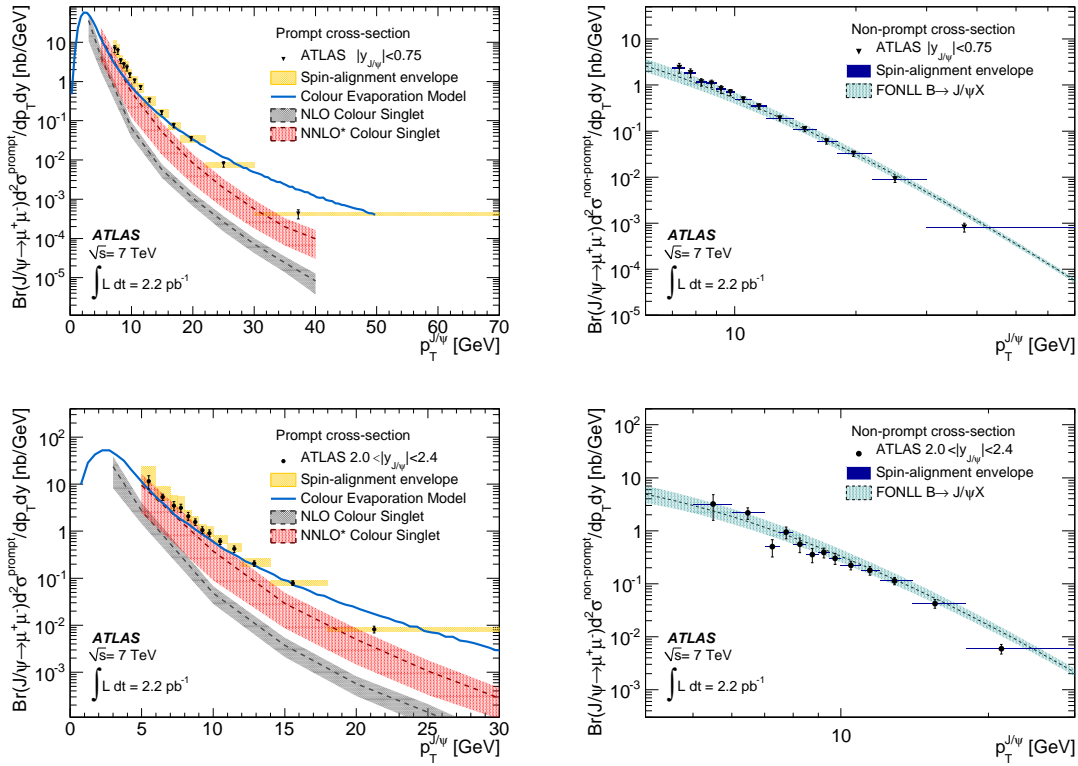


Figure 2: Differential cross-sections of inclusive, prompt and non-prompt J/ψ at $\sqrt{s} = 7 \text{ TeV}$ in two intervals of J/ψ rapidity: $|y(J/\psi)| < 0.75$ at the top and $2.0 < |y(J/\psi)| < 2.4$ at the bottom pictures [3].

so called tagged muons with tracks reconstructed in Inner Detector only and with small energy deposition in calorimeters.

2. J/ψ production in pp -interactions at $\sqrt{s} = 7 \text{ TeV}$

Measurements of J/ψ production cross sections in pp collisions at $\sqrt{s} = 7 \text{ TeV}$ with 2.3 pb^{-1} integrated luminosity are reported in Ref.[3]. The inclusive cross-section is measured in bins of rapidity y and transverse momentum p_T of J/ψ , covering the range $|y| < 2.4$ and $1 < p_T < 70 \text{ GeV}$. The fraction of non-prompt J/ψ mesons is also measured as a function of J/ψ transverse momentum and rapidity and double-differential cross-sections are extracted separately for promptly-produced J/ψ mesons and those coming from B -hadron decays.

It is found that the measurements made by ATLAS and CMS are in good agreement with each other in the overlapping range of moderate p_T values and complement each other at high (ATLAS) and low (CMS) values of transverse momenta. The results are also compared to various theoretical calculations of prompt as well as nonprompt J/ψ production. In general, the theoretical curves describe the non-prompt data well, but significant deviations are observed in the prompt production spectra both in shape and normalisation, particularly at high transverse momenta. The production of prompt J/ψ above $p_t(J/\psi) = 30 \text{ GeV}$ explored for the first time with this measurement.

3. Υ family in pp -interactions at $\sqrt{s} = 7\text{ TeV}$

Differential cross section of $\Upsilon(1S)$ production is published in Ref.[4] (Fig.3). Results are based on an integrated luminosity of 1.13 pb^{-1} . Both muons are required to have $p_t > 4\text{ GeV}$ and absolute pseudorapidity $|\eta| < 2.5$.

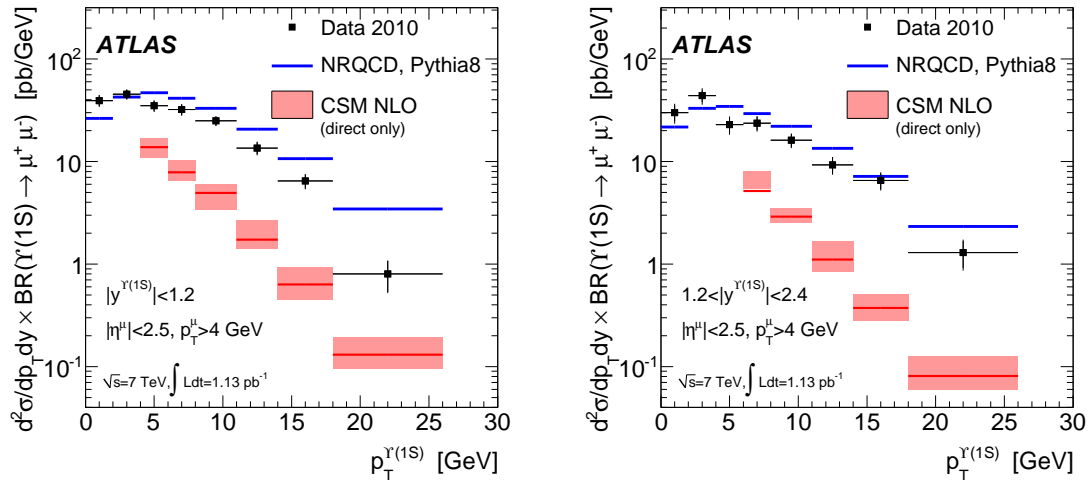


Figure 3: Fiducial Production Cross-Section of $\Upsilon(1S)$ in different rapidity intervals[4].

More details of the study are presented in Ref. [5], based on the statistics corresponding to integrated luminosity of $\sim 1.8\text{ fb}^{-1}$. This measurement provides a test of heavy quarkonium production mechanisms, which is complementary to the J/ψ production and have the following advantages:

- no contributions from B-decays;
- heavier quark mass provides better perturbative convergence.

There are also difficulties,

- more excited states $\Upsilon(1S, 2S, 3S)$ and $\chi_b(nP)$ feed-down contributions add complications,
- larger background contributions, Υ states merge together.

The resolution between $\Upsilon(1S, 2S, 3S)$ states is demonstrated in Fig.4, separately for Barrel ($|\eta| < 1.2$) and Endcap ($1.2 < |\eta| < 2.25$) regions. Fiducial cross sections (at $p_T^\mu > 4\text{ GeV}$ and $|\eta|^\mu < 2.3$) are shown in Fig.5 in two Υ rapidity intervals. The fiducial measurements presented here are precise and free from any assumptions on the angular dependencies of the dimuon system, accurately reflecting the production dynamics in proton-proton collisions at $\sqrt{s} = 7\text{ TeV}$.

Total production cross sections for $p_T < 70\text{ GeV}$ and in the rapidity interval $|y^\Upsilon| < 2.25$ are measured to be, $8.01 \pm 0.02 \pm 0.36 \pm 0.31\text{ nb}$, $2.05 \pm 0.01 \pm 0.12 \pm 0.08\text{ nb}$ and $0.92 \pm 0.01 \pm 0.07 \pm 0.04\text{ nb}$ for $\Upsilon(1S, 2S, 3S)$, respectively, with uncertainties separated into statistical, systematic, and luminosity measurement effects. These cross sections are obtained assuming unpolarized production. If the production polarization is fully transverse or longitudinal with no azimuthal dependence

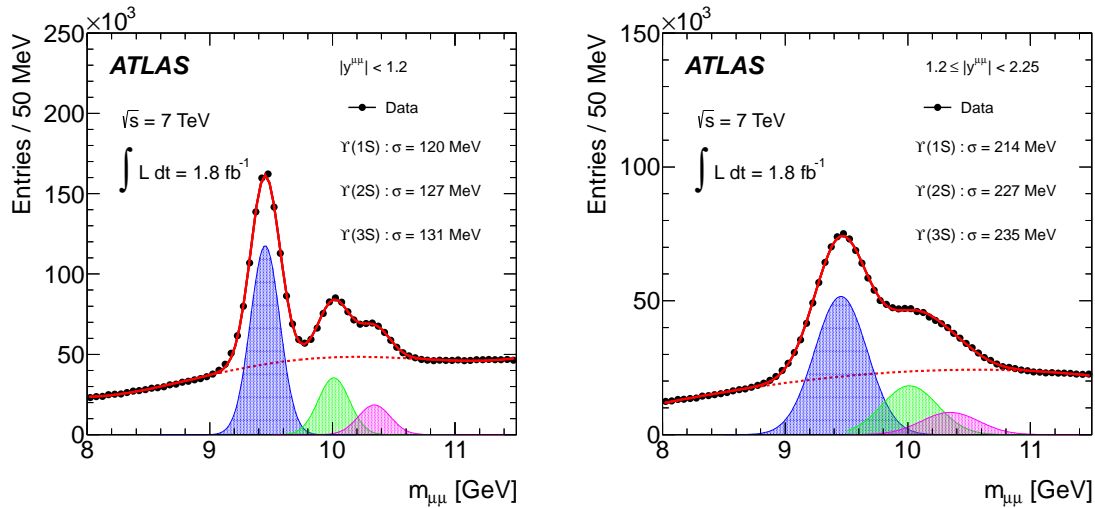


Figure 4: The dimuon invariant mass spectrum for events used in the $\Upsilon(1S)$, $\Upsilon(2S)$, $\Upsilon(3S)$ analysis. Separate spectra are shown for those events with the dimuon candidate (left) in the central region of the detector ($|y^{\mu\mu}| < 1.2$) and (right) in the forward region $1.2 < |y^{\mu\mu}| < 2.25$ [5].

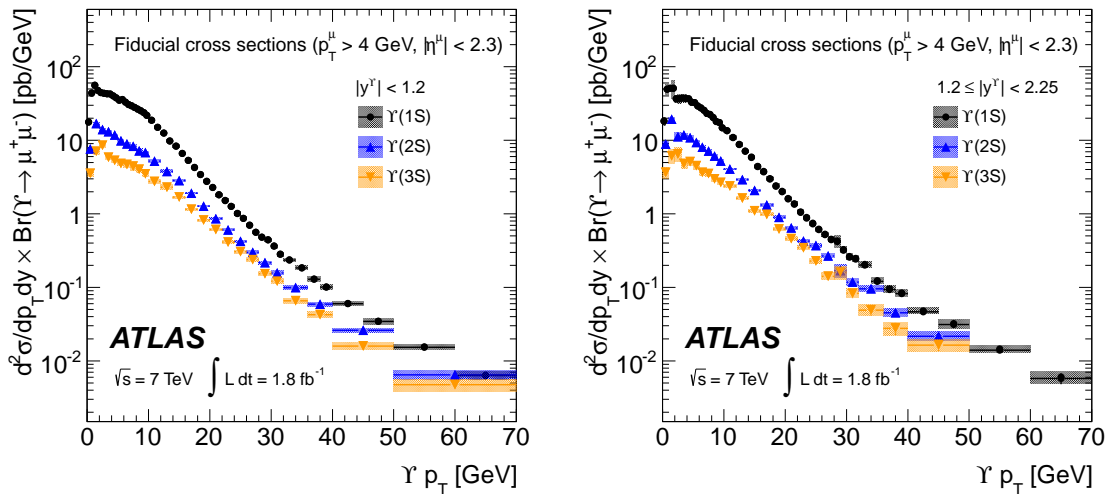


Figure 5: Differential cross sections multiplied by the dimuon branching fraction, for central (left) and forward (right) rapidities, for $\Upsilon(1S)$, $\Upsilon(2S)$ and $\Upsilon(3S)$ production within the fiducial acceptance. Shaded areas correspond to total uncertainties on the measurement, including systematic effects[5].

in the helicity frame, the cross section may vary by approximately $\pm 20\%$. If a nontrivial azimuthal dependence is considered, integrated cross sections may be significantly enhanced by a factor of 2 or more.

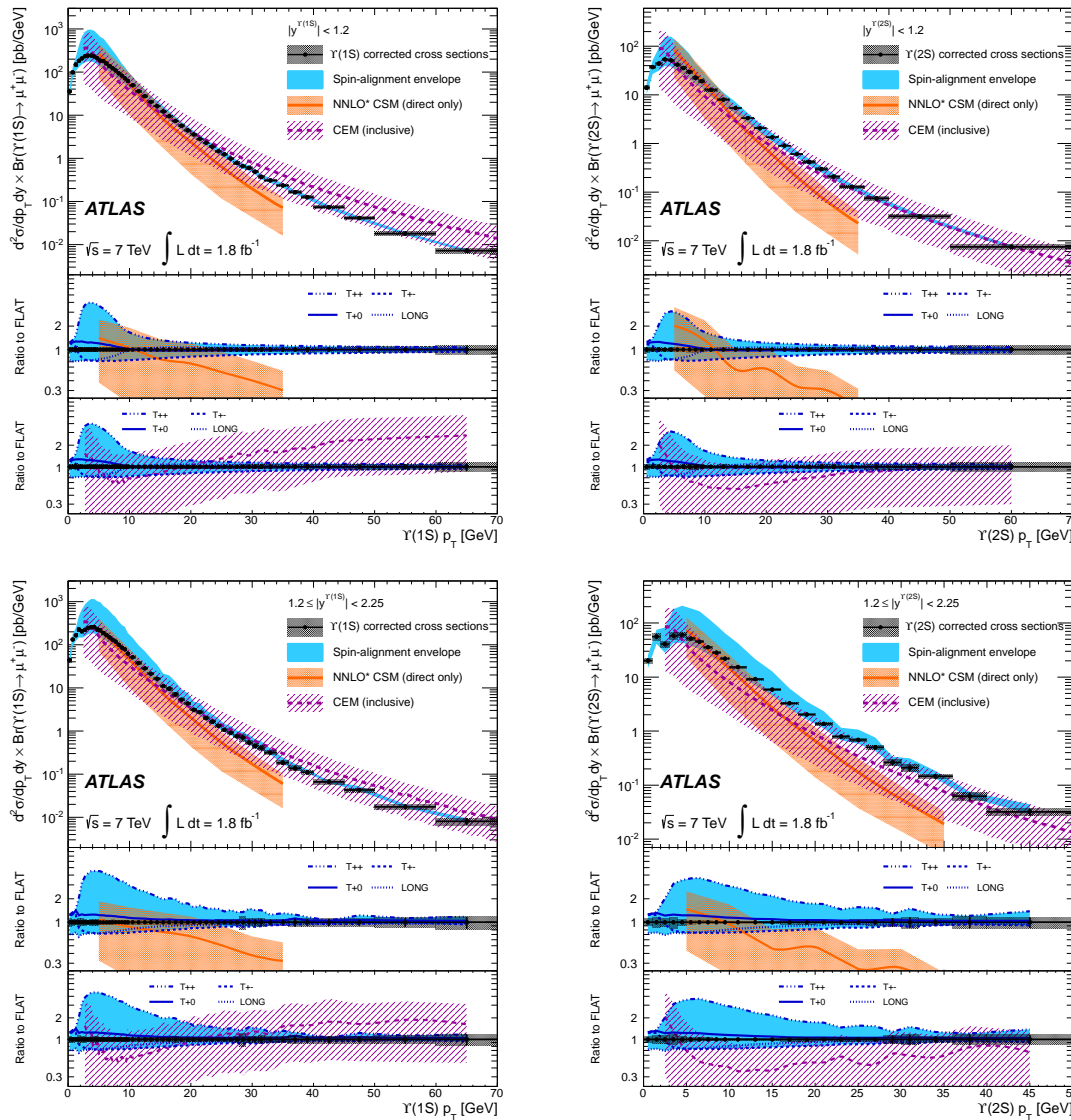


Figure 6: Differential cross sections multiplied by the dimuon branching fraction, for $\Upsilon(1S)$ production extrapolated to the full phase space (left) and $\Upsilon(2S)$ production extrapolated to the full phase space (right). Top and bottom pictures correspond to central and forward regions, respectively. The maximal envelope of variation of the result due to spin-alignment uncertainty is indicated by the solid band. Also shown are predictions of direct production with the $NNLO^*$ color-singlet mechanism (CSM) and inclusive predictions from the color evaporation model (CEM). These theory predictions are shown as a ratio to the data in the lower panes for CEM (middle) and CSM (bottom), along with detail of the variations of the cross section measurement under the four anisotropic spin-alignment scenarios as a ratio to the nominal data[5].

Differential cross sections multiplied by the dimuon branching fraction and extrapolated to the full phase space for (top) central and (bottom) forward rapidities of $\Upsilon(1S)$ and $\Upsilon(2S)$ are shown in Fig.6. Experimental data is compared to two theoretical predictions of Υ production. The first [6] is a QCD-based calculation using the color-singlet mechanism [7], referred to as $NNLO^*$ CSM, and presumes that meson production occurs via a color-singlet state and includes full corrections up to next-to-leading order (NLO), as well as some of the most important next-to-next-to-leading-order (NNLO) terms. This measurement is much more complete than Tevatron or current CMS results, it extends further in $p_t(\Upsilon)$, has small uncertainties and offers a full treatment of the effect of spin-alignment on the observed cross section.

4. $\chi_b \rightarrow \Upsilon(nS) + \gamma$ and $\chi_b(3P)$ discovery

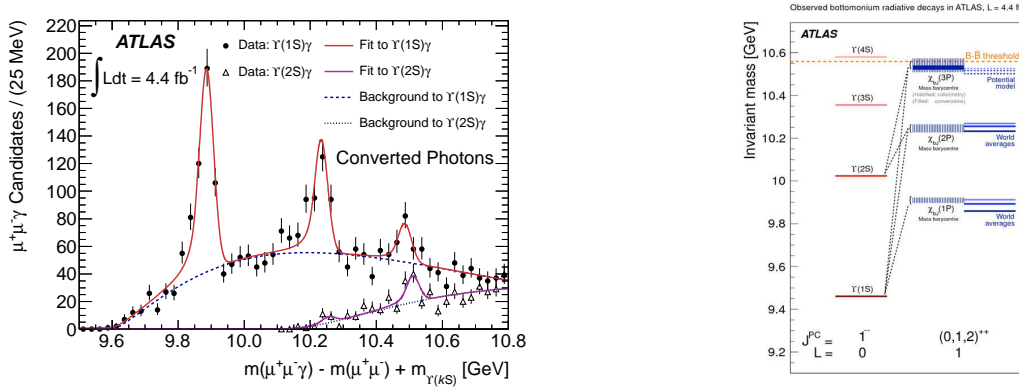


Figure 7: Left picture: The mass distributions of $\chi_b \rightarrow \Upsilon(kS)\gamma$, ($k = 1, 2$) candidates formed using photons which have converted and been reconstructed in the Inner Detector. Data are shown before the correction for the energy loss from the photon conversion electrons due to bremsstrahlung and other processes. The data for decays of $\chi_b \rightarrow \Upsilon(1S) + \gamma$ $\chi_b \rightarrow \Upsilon(2S) + \gamma$ are plotted using circles and triangles, respectively. Solid lines represent the total fit result for each mass window. The dashed lines represent the background components only. Right picture: χ_b family[8].

At the end of 2011 ATLAS discovered a new quark-antiquark bound state, the $\chi_b(3P)$, in mass spectra $\Upsilon(1S) + \gamma$ and $\Upsilon(2S) + \gamma$ (Fig.7 left) [8]. The photon in χ_b study is reconstructed either through conversion to e^+e^- or by direct calorimetric measurement, with the loose photon selection and a minimum photon transverse energy of 2.5 GeV. Data sample used for this study has been acquired at $\sqrt{s} = 7 TeV$ and corresponding to an integrated luminosity of $4.4 fb^{-1}$. Final result is obtained with converted photons, with requirements on $p_t > 0.5 GeV$ for both tracks, a small angle between tracks, a confirmation of e-hypothesis in Transition Radiation Tracker and a distance between reconstructed vertex and the beam axis $> 4 cm$.

The $\chi_b(3P)$ significance is assessed from $\log(L_{max}/L_0)$, where (L_{max}) and (L_0) are the likelihood values from the nominal fit and from a fit with no $\chi_b(3P)$ signal included, respectively. The significance of the $\chi_b(3P)$ signal is found to be in excess of 6 standard deviations in each of the unconverted and converted photon selections independently.

This result is now included in the PDG 2012 (Fig.7 right). Discovery has been confirmed by LHCb and D0:

- ATLAS mass: $10.530 \pm 0.005_{stat} \pm 0.008_{syst} \text{ GeV}$;
- LHCb mass: $10.535 \pm 0.010_{stat} \pm ???_{syst} \text{ GeV}$;
- D0 mass: $10.551 \pm 0.014_{stat} \pm 0.017_{syst} \text{ GeV}$;

The ATLAS result remains most precise. Production cross section and properties measurements are ongoing. Notice that the expected superfine splitting for new state is of order of 20 MeV and cannot be resolved with available experimental precision.

5. b -hadron production cross section at $\sqrt{s} = 7 \text{ TeV}$

The b -hadron production cross section is measured with the ATLAS detector in pp collisions at $\sqrt{s} = 7 \text{ TeV}$, using 3.3 pb^{-1} of integrated luminosity, collected during the 2010 LHC run [9]. The b -hadrons are selected by partially reconstructing $D^{*+}\mu^{-}X$ final states (Fig.8). Differential cross sections are measured as functions of the transverse momentum and pseudorapidity. The measured production cross section for a b -hadron with $p_T > 9 \text{ GeV}$ and $|\eta| < 2.5$ is $32.7 \pm 0.8(stat.)_{-6.8}^{+4.5}(syst) \mu b$, higher than the next-to-leading order QCD predictions but consistent within the experimental and theoretical uncertainties..

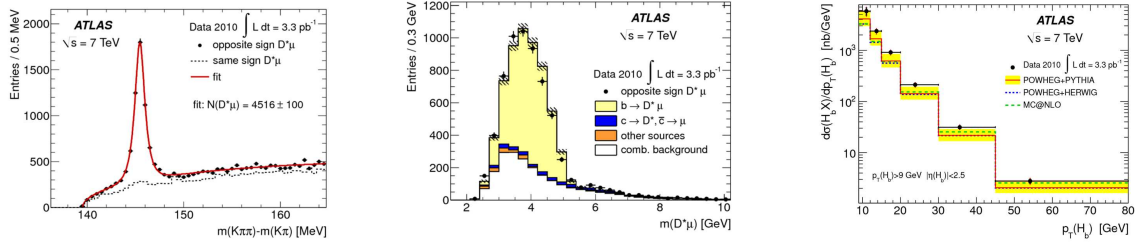


Figure 8: Left: Distribution of the mass difference Δm for $D^*\mu$ combinations of opposite charge (points) and same charge (dashed line). Center: Distribution of the opposite charge $D^*\mu$ invariant mass, for mass combinations within $\pm 3\sigma$ of the Δm peak. Right: Differential cross section for b -hadron production as a function of p_T [9].

6. Measurement of Λ_b lifetime and mass

A measurement of the Λ_b^0 lifetime and mass was performed in the decay channel $\Lambda_b^0 \rightarrow J/\psi(\mu^+\mu^-)\Lambda(p\pi^-)$ [10]. The analysis uses a signal sample of about 2200 Λ_b^0 and $\bar{\Lambda}_b^0$ decays that are reconstructed in 4.9 fb^{-1} of ATLAS pp collision data collected in 2011 at the LHC center-of-mass energy of 7 TeV . A simultaneous mass and decay time maximum likelihood fit is used to extract the Λ_b^0 lifetime and mass. They are measured to be $\tau_{\Lambda_b} = 1.449 \pm 0.036(stat) \pm 0.017(syst) \text{ ps}$ and $m_{\Lambda_b} = 5619.7 \pm 0.7(stat) \pm 1.1(syst) \text{ MeV}$. Projections of two-dimensional fit on mass and time axes are shown in Fig.9. Compilations of available measurements of Λ_b^0 mass and lifetime shown in Fig.10. The ATLAS lifetime measurement better than the existing best measurements. The ATLAS mass measurement compares well with recent LHCb result of $5919.19 \pm 0.7 \pm 0.3 \text{ MeV}$ and is the second best measurement, reducing uncertainty in the world average from 0.7 to 0.6 MeV [11].

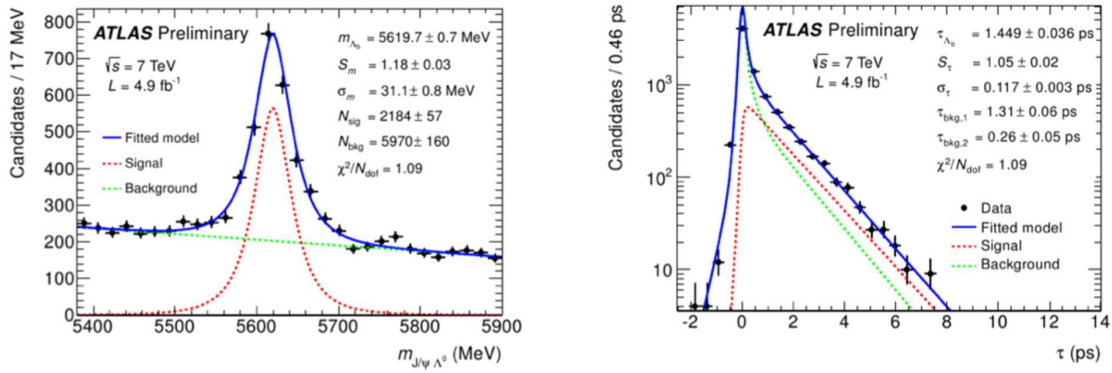


Figure 9: Projections of the fitted probability density function (PDF) onto the mass (left panel) and the proper decay time (right panel) axes for Λ_b^0 b candidates[10].

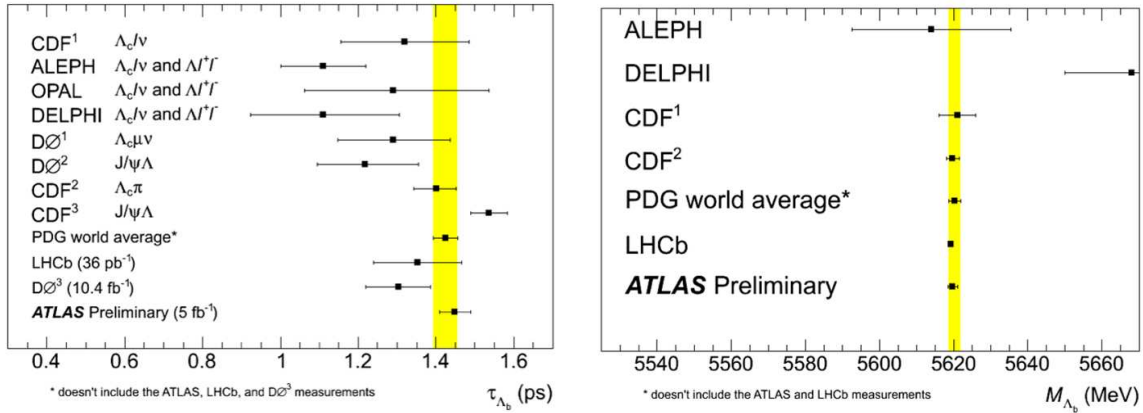


Figure 10: Compilations of available Λ_b^0 lifetime (left) and mass (right) measurements[10, 11].

7. Limit on branching $B_s \rightarrow \mu^+ \mu^-$

A limit on the branching fraction $BR(B_s \rightarrow \mu^+ \mu^-)$ is set using 2.4 fb^{-1} of integrated luminosity collected in 2011 [12]. The process $B^\pm \rightarrow J/\psi K^\pm$, with $J/\psi \rightarrow \mu^+ \mu^-$ is used as a reference channel for the normalization of integrated luminosity, acceptance and efficiency. The final selection is based on a multivariate analysis performed on three categories of events determined according to their mass resolution (the largest pseudorapidity value of two muons $|\eta_{max}| < 1.0$, $1.0 < |\eta_{max}| < 1.5$, $1.5 < |\eta_{max}| < 2.5$), yielding a limit of $BR(B_s \rightarrow \mu^+ \mu^-) < 2.2(1.9) \times 10^{-8}$ at 95%(90%) confidence level. Comparison with similar studies in CMS and LHCb experiments can be found in [13]. The combination results in upper limits on the branching fractions $BR(B_s \rightarrow \mu^+ \mu^-) < 4.2 \times 10^{-9}$ and $BR(B_d \rightarrow \mu^+ \mu^-) < 8.1 \times 10^{-10}$, both at 95% confidence level.

The next step in the ATLAS analysis is to double statistics with the full 2011 data, with hope to gain more than a $\sim \sqrt{2}$ improvement on sensitivity due to modifications in the analysis.

In the 2012 data, the number of events per inverse femtobarn drops due to stricter trigger requirements, therefore the expected improvement is less than the rise in \sqrt{lumi} , but further analysis

improvements are expected.

8. Study of CP -violation in $B_s \rightarrow J/\psi\phi(1020) \rightarrow J/\psi K^+ K^-$ decay

This decay proceeds in S , P and D -waves, leading to CP -even final state in S and D -waves and to CP -odd state in P -wave decay. CP violation arises from interference of $B_s \rightarrow J/\psi\phi$ decay and $B_s - \bar{B}_s$ mixing and it is proportional to a phase difference, ϕ_s , of the two complex weak amplitudes. The SM predicted value for this angle is small, $\phi_s = 0.0363 \pm 0.0017$ rad, currently not accessible by any experiment with available data. However it is within LHC potential with future improvements. Many New Physics models predict enhancements of ϕ_s . Searches started at Tevatron and continue at LHC. ϕ_s can be extracted from $B_s \rightarrow J/\psi\phi$ data by time-dependent angular analysis without tagging the b/\bar{b} quark at the production time.

B_s mixing is described in the lowest order by box diagrams, involving two W and two up-type quarks. This leads to two mass eigenstates (Light and Heavy) which have different lifetimes. In the neutral B_s system, the two mass eigenstates have similar lifetimes and must be studied together. This is different from the neutral Kaon system, where the two mass eigenstates have very different lifetimes (by a factor ~ 600).

The final state $J/\psi\phi$ is a mixture of CP -even ($\sim 75\%$) and CP -odd ($\sim 25\%$) states. The ϕ_s angle can only be measured if CP -states are separated using angular distributions of final state particles (there are two polar decay angles in J/ψ and ϕ rest frames and one azimuth angle between the two decay planes).

Details of the untagged analysis can be found in Ref.[14]. There are ten time-dependent amplitudes in the signal probability distribution function, four amplitudes corresponding to S , P , D waves with ϕ resonance and a small ($\sim 2\%$) P -wave with $(K^+ K^-)$ system in S -wave, and six interference terms. The amplitudes include three weak parameters [ϕ_s , $\Delta\Gamma = (\Gamma_H - \Gamma_L)$, $\Gamma = (\Gamma_H + \Gamma_L)/2$] and two strong phases. Without tagging and for small ϕ_s values, one of the strong phases (ϕ_\perp in the transversity notation) cannot be well measured, so a Gaussian constraint to the best measured value, (2.95 ± 0.39) rad [15] was applied for this parameter. This measurement of ϕ_\perp phase was done by LHCb experiment. Other phases are measured by ATLAS.

A sample of $\sim 23k$ reconstructed $J/\psi\phi$ events acquired in 2011 at $\sqrt{s} = 7 TeV$ used in this analysis. The results are consistent with the world average values and with theoretical expectations:

- $\phi_s = 0.22 \pm 0.41 \pm 0.10$ rad;
- $\Delta\Gamma_s = 0.053 \pm 0.021(stat) \pm 0.010(syst) ps^{-1}$;
- $\Gamma_s = 0.677 \pm 0.007(stat) \pm 0.004(syst) ps^{-1}$.

Projections of two-dimensional fit on mass and time axes are shown in Fig.11. Compilation of measurements of CP -violating parameters in $B_s \rightarrow J/\psi\phi$ decay presented in Fig.12. One can see, that the ϕ_s measurement in ATLAS is less precise in comparison with LHCb, but the ATLAS precision in lifetime measurements is well competitive.

Significant improvements in the precision are expected in near future, from inclusion of the b/\bar{b} tagging (in preparation) and the 2012 data.

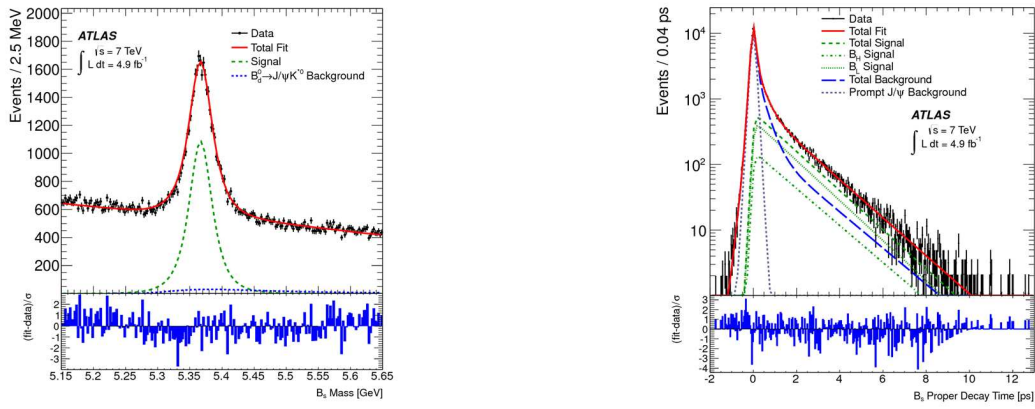


Figure 11: Projections of the fitted probability density function (PDF) onto the mass (left panel) and the proper decay time (right panel) axes for $B_s \rightarrow J/\psi\phi$ candidates[14].

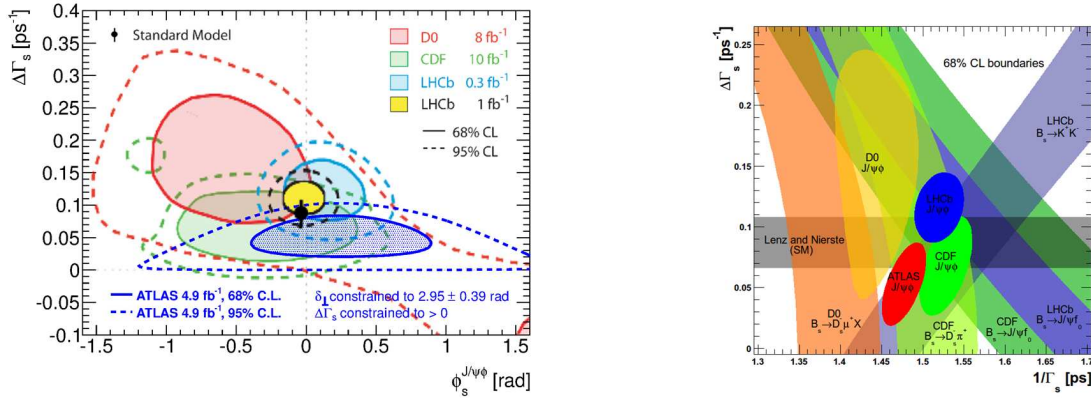


Figure 12: Compilation of measurements of CP -violating parameters in $B_s \rightarrow J/\psi\phi$ decay: $\Delta\Gamma$ vs ϕ_s (left picture)[16]; $\Delta\Gamma$ vs Γ (right picture)[16].

9. Conclusions

B-physics at LHC is rich, and ATLAS experiment has produced competitive results in several fields, including spectroscopy, lifetime measurements and untagged analysis of CP -violation in B_s decays. Work on the B-tagging methods in ATLAS is ongoing.

Many other analyses which were not mentioned in this talk are in progress, for example the $\psi(2s)$ production, associated production of W-boson plus prompt J/ψ , $X(3772)$ study, B^\pm cross section measurement, search of excited B_c states and $B_c \rightarrow D_s^{(*)} \mu^+ \mu^-$ decay.

References

[1] The ATLAS Experiment at the CERN Large Hadron Collider. ATLAS Collaboration, 2008 JINST 3 S08003.

202007

- [2] ATLAS Collaboration,
<https://twiki.cern.ch/twiki/bin/view/AtlasPublic/BPhysPublicResults>;
- [3] Measurement of the differential cross-sections of inclusive, prompt and non-prompt J/ψ production in pp collisions at $\sqrt{s} = 7\text{ TeV}$, ATLAS Collaboration, Nucl.Phys. B850 (2011) 387;
- [4] $\Upsilon(1S)$ Fiducial Production Cross-Section of $Upsilon(1S)$ in pp collisions at $\sqrt{s} = 7\text{ TeV}$ in ATLAS, ATLAS Collaboration, Phys.Lett. B705 (2011) 9;
- [5] Measurement of Upsilon production in 7 TeV pp collisions at ATLAS, ATLAS Collaboration, Phys. Rev. D87 (2013) 052004, CERN-PH-EP-2012-295;
- [6] P. Artoisenet, J. M. Campbell, J. P. Lansberg, F. Maltoni, and F. Tramontano, Phys.Rev.Lett. 101 (2008) 152001; J. P. Lansberg, Eur. Phys. J. C 61, 693 (2009).
- [7] J. F. Owens, E. Reya, and M. Gluck, Phys. Rev. D 18, 1501 (1978); V.G. Kartvelishvili, A. K. Likhoded, and S. R. Slabospitsky, Yad. Fiz. 28, 1315 (1978) [Sov. J. Nucl. Phys. 28, 678 (1978)]; C. H. Chang, Nucl. Phys. B172, 425 (1980); E. L. Berger and D. L. Jones, Phys. Rev. D 23, 1521 (1981); R. Baier and R. Ruckl, Nucl. Phys. B201, 1 (1982); Z. Phys. C 19, 251 (1983).
- [8] Observation of a new χ_b state in radiative transitions to $\Upsilon(1S)$ and $\Upsilon(2S)$ at ATLAS, ATLAS Collaboration, Phys.Rev.Lett. 108 (2012) 152001;
- [9] Measurement of the b -hadron production cross section using decays to $D^{*+}\mu^-X$ final states in pp -collisions at $\sqrt{s} = 7\text{ TeV}$ with the ATLAS detector, ATLAS Collaboration, Nucl. Phys. B 864 (2012) 341;
- [10] Measurement of the Λ_b lifetime and mass in the ATLAS experiment, ATLAS Collaboration, Phys. Rev. D87 (2013) 032002, arXiv:1207.2284 [hep-ex];
- [11] Review of Particle Physics, Beringer et al. (Particle Data Group), Phys. Rev. D86 (2012) 010001;
- [12] Search for the decay $B_s \rightarrow \mu^+\mu^-$ with the ATLAS detector, ATLAS Collaboration, Phys.Lett. B713, (2012) 387, arXiv:1204.0735 [hep-ex];
- [13] Combined LHC limit to the decay $B_s \rightarrow \mu^+\mu^-$ ATLAS,CMS and-LHCb Collaborations, ATLAS-CONF-2012-061 note, <https://cds.cern.ch/record/1456262>;
- [14] Time-dependent angular analysis of the decay $B_s^0 \rightarrow J/\psi\phi$ and extraction of $\Delta\Gamma$ and the CP-violating weak phase, ATLAS Collaboration, JHEP 1212 (2012) 072, arXiv:1208.0572 [hep-ex]
- [15] LHCb collaboration, R. Aaij et al., Measurement of the CP-violating phase ϕ_s in the decay $B_s \rightarrow J/\psi\phi$, Phys. Rev. Lett. 108 (2012) 101803 [arXiv:1112.3183];
- [16] ATLAS Collaboration,
<https://atlas.web.cern.ch/Atlas/GROUPS/PHYSICS/PAPERS/BPHY-2011-05>;